DIRECT NUMERICAL SIMULATION OF THE 3D STRATIFIED VISCOUS FLUID FLOWS AROUND A SPHERE

Pavel V. Matyushin and Valentin A. Gushchin

Institute for Computer Aided Design of the Russian Academy of Sciences
19/18, 2nd Brestskaya str., Moscow 123056, Russia
e-mail: pmatyushin@mail.ru, gushchin@icad.org.ru

Key words: stratified fluid; sphere wake; direct numerical simulation; vortex structures; visualization; internal waves.

Abstract. *At the present paper for the first time the continuous changing of the complex 3D vortex structure of the flow around a sphere (moving in the stratified incompressible viscous fluid) with increasing of the stratification is demonstrated using a β-visualization of the 3D vortex structures (the internal waves and the sphere wake). The velocity fields used for the β-visualization were obtained by means of the direct numerical simulation (DNS) on the basis of the Navier-Stokes equations in the Boussinesq approximation on the massive parallel computers with a distributed memory at the following ranges of the internal Froude Fr and Reynolds Re numbers: 0.004 ≤ Fr ≤ 100, 10 ≤ Re ≤ 500 (Fr = U/(N·d), Re = U·d/ν, where U is the scalar of the sphere velocity, N is a buoyancy frequency, d is a sphere diameter and ν is the kinematical viscosity). The classification of the stratified flow regimes derived from our simulation is more close to [1]. A brief description of the used numerical method, the β-visualization technique and the flow regimes for the homogeneous fluid are given.*

1 INTRODUCTION

Unsteady 3D separated and undulatory fluid flows around a moving blunt body are very wide spread phenomena in the nature. The understanding of such flows is very important both from theoretical and from practical points of view. In the experiments the 2D internal waves structure in the vertical plane and the 3D vortex structure of the wake are observed [1-3]. Using DNS the full 3D vortex structures of the flow (the 3D internal waves and the 3D wake) can be observed. The numerical studies of the non-homogeneous (stratified) fluids are very rare [4-5]. In this connection at the present paper the stratified viscous fluid flows around a sphere are investigated by means of DNS on the basis of the Navier-Stokes equations in the Boussinesq approximation on the massive parallel computers with a distributed memory at the following ranges of the main flow parameters: $0.004 \leq Fr \leq 100$, $10 \leq Re \leq 500$.

2 NUMERICAL METHOD SMIF

The paper must be written in English within a printing box of 16 cm x 24 cm, centered in the page. The paper including figures, tables and references must have a minimum length of 4 pages and must not exceed 20 pages. Maximum file size is 6 MB.

2.1 Equations and boundary conditions

Let $\rho(x, y, z) = \rho_0(1 - x/(2C) + S(x, y, z))$ is the density of the linearly stratified fluid where x, y, z are the Cartesian coordinates; z, x, y are the streamwise, lift and lateral directions (x, y, z have been non-dimensionalized by $d/2$); $C = \Lambda/d$ is the scale ratio, Λ is the buoyancy scale, which is related to the buoyancy frequency N and period T_b ($N = 2\pi/T_b$, $N^2 = g/\Lambda$); g is the scalar of the gravitational acceleration; S is a dimensionless perturbation of salinity. The density stratified viscous fluid flows have been simulated on the basis of the Navier-Stokes equations in the Boussinesq approximation (1) – (3) (including the diffusion equation (3) for the stratified component (salt)) with four dimensionless parameters: Fr, Re, $C \gg 1$, $Sc = \nu/\kappa = 709.22$, where κ is the salt diffusion coefficient.

$$\frac{\partial \mathbf{v}}{\partial t} + (\mathbf{v} \cdot \nabla)\mathbf{v} = -\nabla p + \frac{2}{Re}\Delta \mathbf{v} + \frac{C}{2Fr^2}S\frac{\mathbf{g}}{g} \tag{1}$$

$$\nabla \cdot \mathbf{v} = 0 \tag{2}$$

$$\frac{\partial S}{\partial t} + (\mathbf{v} \cdot \nabla)S = \frac{2}{Sc \cdot Re}\Delta S + \frac{v_x}{2C} \tag{3}$$

In (1) – (3) $\mathbf{v} = (v_x, v_y, v_z)$ is the velocity vector (non-dimensionalized by U), p is a perturbation of pressure (non-dimensionalized by $\rho_0 U^2$).

The spherical coordinate system R, θ, φ ($x = R\sin\theta\cos\varphi$, $y = R\sin\theta\sin\varphi$, $z = R\cos\theta$, $\mathbf{v} = (v_R, v_\theta, v_\varphi)$) and O-type grid are used. On the sphere surface the following boundary conditions have been used:

$$v_R = v_\theta = v_\varphi = 0, \quad \left.\frac{\partial \rho}{\partial R}\right|_{R=d/2} = \left.\left(\frac{\partial S}{\partial R} - \frac{1}{2C}\frac{\partial x}{\partial R}\right)\right|_{R=d/2} = 0$$

On the external boundary of the O-type grid the following boundary conditions have been used: 1) for $z < 0$: $v_R = \cos\theta$, $v_\theta = -\sin\theta$, $v_\varphi = 0$, $S = 0$; 2) for $z \geq 0$: $v_R = \cos\theta$, $v_\theta = -\sin\theta$, $\partial v_\varphi/\partial R = 0$, $\partial S/\partial z = 0$.

For solving of the Navier-Stokes equations (1) – (3) the Splitting on physical factors Method for Incompressible Fluid flows (SMIF) with the hybrid explicit finite difference

scheme (second-order accuracy in space, minimum scheme viscosity and dispersion, monotonous, capable for work in the wide range of the Reynolds and Froude numbers) based on the Modified Central Difference Scheme (MCDS) and the Modified Upwind Difference Scheme (MUDS) with the special switch condition depending on the velocity sign and the sign of first and second differences of the transferred functions has been used [6].

2.2 Splitting scheme of SMIF

Let the velocity, the perturbation of pressure and the perturbation of salinity are known at some moment $t_n = n \cdot \tau$, where τ is time step, and n is the number of time-steps. Then the calculation of the unknown functions at the next time level $t_{n+1} = (n+1) \cdot \tau$ for equations (1) – (3) can be presented in the following four-step form:

Step I:
$$\frac{\tilde{\mathbf{v}} - \mathbf{v}^n}{\tau} = -(\mathbf{v}^n \cdot \nabla)\mathbf{v}^n + \frac{2}{Re}\Delta\mathbf{v}^n + \frac{C}{2Fr^2}S^n\frac{\mathbf{g}}{g}$$

Step II:
$$\tau\Delta p = \nabla \cdot \tilde{\mathbf{v}}$$

Step III:
$$\frac{\mathbf{v}^{n+1} - \tilde{\mathbf{v}}}{\tau} = -\nabla p$$

Step IV:
$$\frac{S^{n+1} - S^n}{\tau} = -(\mathbf{v}^{n+1} \cdot \nabla)S^n + \frac{2}{Sc \cdot Re}\Delta S^n + \frac{v_x^{n+1}}{2C}$$

The Poisson equation for the pressure (step II) has been solved by the diagonal Preconditioned Conjugate Gradients Method.

2.3 Finite-difference scheme for the convective terms of the equations (1)-(3) (1D example)

Let us consider the linear model equation:
$$f_t + u f_x = 0, \qquad u = const. \tag{4}$$

Let
$$\frac{f_i^{n+1} - f_i^n}{\tau} + u\frac{f_{i+\frac{1}{2}}^n - f_{i-\frac{1}{2}}^n}{h} = 0 \tag{5}$$

be a finite-difference approximation of equation (4).

Let us investigate the class of the difference scheme which can be written in the form of the two-parameter family which depends on the parameters α and β in the following manner:

$$f_{i+\frac{1}{2}}^n = \begin{cases} \alpha f_{i-1}^n + (1-\alpha-\beta)f_i^n + \beta f_{i+1}^n, & u \geq 0 \\ \alpha f_{i+2}^n + (1-\alpha-\beta)f_{i+1}^n + \beta f_i^n, & u < 0. \end{cases} \tag{6}$$

In this case the first differential approximation for equation (5) has the form

$$f_t + uf_x = \left[\frac{h}{2}|u|(1 + 2\alpha - 2\beta) - \frac{\tau u^2}{2}\right]f_{xx}. \tag{7}$$

If we put $\alpha = \beta = 0$ in (6) we'll obtain usual first order monotonic scheme which is stable when

$$0 < C = \frac{\tau|u|}{h} \leq 1, \quad \text{where } C \text{ is the Courant number.} \tag{8}$$

If $\alpha = 0$, $\beta = 0.5$ we'll obtain the usual central difference scheme, and for $\alpha = -0.5$, $\beta = 0$ – the usual upwind scheme. Both last two scheme have second order of accuracy in space variable and are non-monotonic.

It is known that it is impossible to construct a homogeneous monotonic difference scheme of higher order than the first order of the approximation for equation (4). A monotonic scheme of higher order can therefore only be constructed either on the basis of second-order homogeneous scheme using smoothing operators, or on the basis of hybrid schemes using different switch conditions from one scheme to another (depending on the nature of the solution), possibly with the use of smoothing.

Here we consider a hybrid monotonic difference scheme based on a combination of a MCDS and MUDS with special switch condition.

Let us investigate schemes with upwind differences, i.e. $\beta = 0$. The requirement that the scheme viscosity should be a minimum, as can readily be seen from equation (7), impose the following condition on α:

$$\alpha = -0.5 \, (\, 1 - C \,). \tag{9}$$

For schemes with $\alpha = 0$, the analogous condition is

$$\beta = 0.5 \, (\, 1 - C \,). \tag{10}$$

Since an explicit finite difference scheme considered, we shall restrict the subsequent analysis to the necessary condition for stability in the case of the explicit schemes (8).

Let us assume that there is a monotonic net function f_i^n, for example, $\Delta f_{i+\frac{1}{2}}^n \equiv f_{i+1}^n - f_i^n \geq 0$ at any i.

The function f_i^{n+1} will also be monotonic when the following conditions are satisfied:
(a) for a scheme with $\beta = 0$ and α from relationship (9), under the condition

$$\Delta f_{i+\frac{1}{2}}^n \leq \zeta(C)\Delta f_{i-\frac{1}{2}}^n, \text{ where } \zeta(C) = 0.5 \, (1 - C) \, / \, (2 - C);$$

(b) for a scheme with $\alpha = 0$ and β from relationship (10), under the condition

$$\Delta f_{i+\frac{1}{2}}^n \leq \sigma(C)\Delta f_{i-\frac{1}{2}}^n, \text{ where } \sigma(C) = 2 \, (\, 1 + C \,) \, / \, C.$$

It can be seen from this that the domains of monotonicity of the homogeneous scheme being considered have a non-empty intersection. Hence, a whole class of hybrid schemes is distinguished by the condition of switching over from one homogeneous scheme to another. The general form of this condition is as follows:

$$\Delta f_{i+\frac{1}{2}}^n = \delta\Delta f_{i-\frac{1}{2}}^n, \quad \text{where } \zeta(C) \leq \delta \leq \sigma(C).$$

The choice of $\delta = 1$ corresponds to the points of the interchange of the sign of the second difference f_i^n and makes it possible to obtain the estimate $f_{xx} = O(h)$ for the required function f at the intersection points, by means of which a second-order approximation is retained with respect to the spatial variables of smooth solutions. We used the following switching condition:

if $\ (u\Delta f\Delta^2 f)_{i+\frac{1}{2}}^n \geq 0,$ then the scheme with $\beta = 0$ (MUDS) is used;

if $(u\Delta f \Delta^2 f)_{i+\frac{1}{2}}^n < 0$, then the scheme with $\alpha = 0$ (MCDS) is used;

where $\Delta^2 f_{i+\frac{1}{2}}^n = \Delta f_{i+1}^n - \Delta f_i^n$.

On smooth solutions this scheme has a second order of approximation with respect to the time and spatial variables. It is stable when the Courant criterion (8) is satisfied and monotonic. More over it was shown that this hybrid scheme comes nearest to the third order schemes.

The generalization of the considered finite-difference scheme for 2D and 3D problems is easily performed for convective terms in (1), (3). For the approximation of other space derivatives in equations (1) – (3) the central differences are used.

The efficiency of the method SMIF and the greater power of supercomputers make it possible adequately to model the three-dimensional separated incompressible viscous flows past a sphere and a circular cylinder at moderate Reynolds numbers [7]-[11] and the air, heat and mass transfer in the clean rooms.
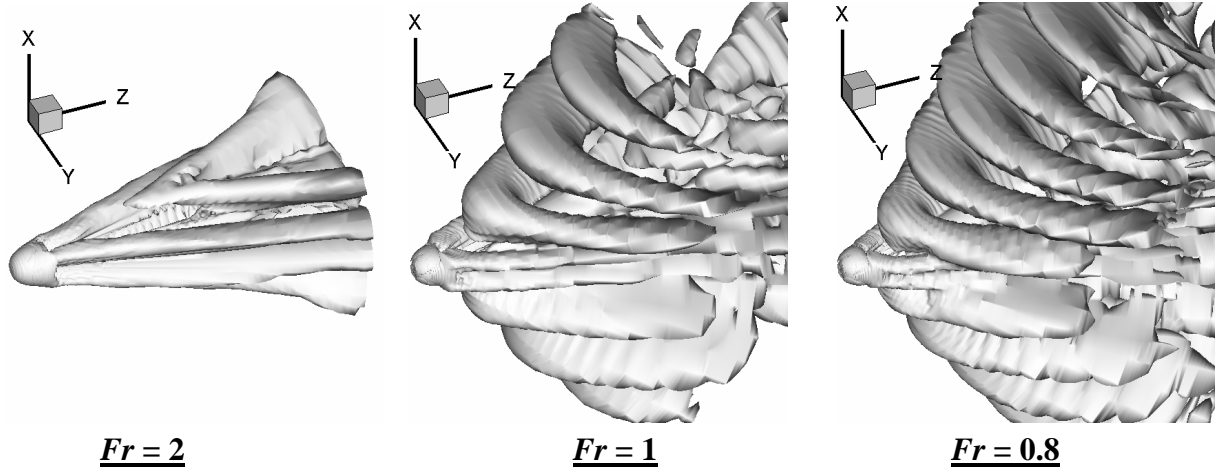

_Fr = 2_   **_Fr = 1_**   **_Fr = 0.8_**

Figure 1: The vortex structures in the stratified fluid around a moving sphere
at *Re* = 100, *Fr* = 2, 1, 0.8 - the isosurfaces β = 0.005,
β is *the imaginary part of the complex-conjugate eigen-values of the velocity gradient tensor* [12]).

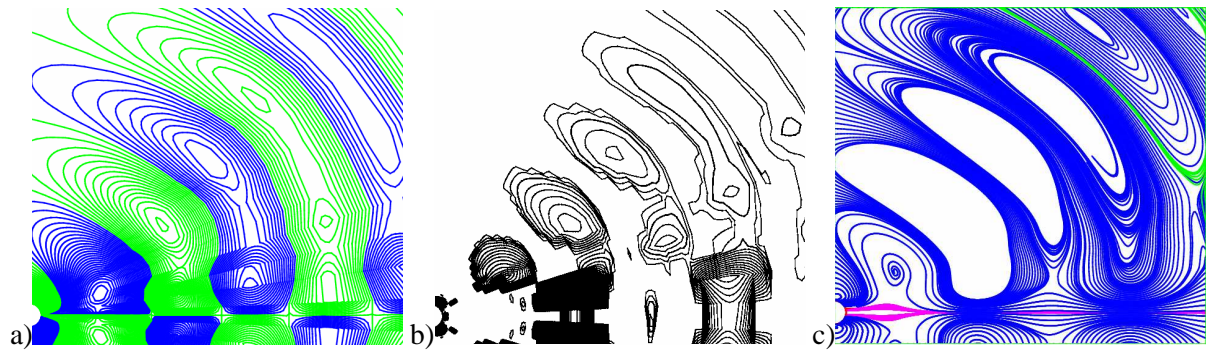

Figure 2: *Re* = 100, *Fr* = 1: a) the isolines of the perturbation of salinity; b) the isolines of β [12];
c) the stream lines in the vertical plane (in the reference frame connected with fluid).

3   THE VISUALIZATION TECHNIQUE

For the visualization of the 3D vortex structures in the sphere wake the isosurfaces of β have been drawing, where β is *the imaginary part of the complex-conjugate eigen-values of the velocity gradient tensor* **G** [12] (fig. 1). β has a real physical meaning. Let us consider a local stream lines pattern around any point in a flow (where β > 0) in a reference frame **x**

moving with the velocity of this point ($\mathbf{v} = d\mathbf{x}/dt \approx \mathbf{G}\,\mathbf{x}$, where $\mathbf{v}$ is a velocity of a fluid particle in the considered reference frame $\mathbf{x}$ and t is time). It's easy to demonstrate (see the theory of the ordinary differential equations) that the local stream lines pattern in the considered reference frame $\mathbf{x}$ is closed or spiral, and β *is the angular velocity of this spiral motion*. The good efficiency of this β-visualization technique has been demonstrated in [11]. The clear relationship between the isolines of the perturbation of the salinity in the vertical plane (the traditional way of the representation of the internal waves (fig. 2a, 3e)) and the horizontal arc-shaped vortex structures (the new 3D way of the representation of the internal waves) is shown at fig. 2.

4   RESULTS

4.1   The diffusion-induced flow around a resting sphere

In the beginning the code for DNS of the 3D separated stratified viscous fluid flows around a sphere has been tested in the case of a resting sphere in a continuously stratified fluid. As a result of this test it was shown (*for the first time*) that the interruption of the molecular flow (by the resting sphere) not only generates the axisymmetrical flow on the sphere surface (from the equator to the poles) but also creates the short unsteady internal waves [13]-[14]. At first a number of these waves is equal to t/T_b. For example at $t = 2 \cdot T_b$ four convective cells with the opposite directions of the vorticity (two waves) are presented in the stream lines distribution. A base cell, whose size is determined by the radius of the sphere, is located near the sphere surface. At time more than $37 \cdot T_b$ the sizes and arrangement of cells are stabilized, and only the base cell and two thin adjacent cells with a thickness 2.2 mm are observed both in the salinity perturbation field S and in the stream lines pattern. In other words *the high gradient sheets of density* with a thickness 2.2 mm are observed near the poles of the resting sphere. The maximum velocity of this quasi-steady flow near the sphere surface is equal to 0.006 mm/s. The similar high gradient sheets of density have been observed before a moving sphere (near the poles) at $Fr \leq 0.1$.

4.2   The classification of the flow regimes around a sphere moving in the viscous stratified fluid

For **flow regime I** ($Fr > 10$ – "*the homogeneous case*") the following sub-classification has been observed previously (see [11]): 1) $Re \leq 200$ – a steady axisymmetrical wake; 2) $200 < Re \leq 270$ – a steady double-thread wake (fig. 4a); 3) $270 < Re \leq 400$ – a procession of the vortex loops (facing upwards), the periodical separation from the one edge of the vortex sheet; 4) $Re > 400$ – the periodical separation from the opposite edges of the irregularly rotating vortex sheet. In this case the following main vortex structures of the flow can be selected: 1) the deformed vortex ring (or semi-rings) in the recirculation zone; 2) the vortex sheet surrounding the recirculation zone; 3) the vortex threads or loops connected with the recirculation zone (see [11]) (fig. 4a). *Owing to our previous investigations* (see [11]) the detailed formation mechanisms of vortices (FMV) in the sphere wake have been described for $200 \leq Re \leq 1000$. In particular it was shown that the detailed FMV for $270 < Re \leq 290$, $290 < Re \leq 320$ and $320 < Re \leq 400$ are different. (The main differences have been observed in the recirculation zone.)

For **flow regime II** ($1.5 \leq Fr \leq 10$ – "*the quasi-homogeneous case* (with four additional threads connected with the vortex sheet surrounding the sphere, fig. 1, 3 (left fig.)") the boundaries of the analogous sub-regimes (flattened in vertical direction and with four additional threads) are slightly shifted.
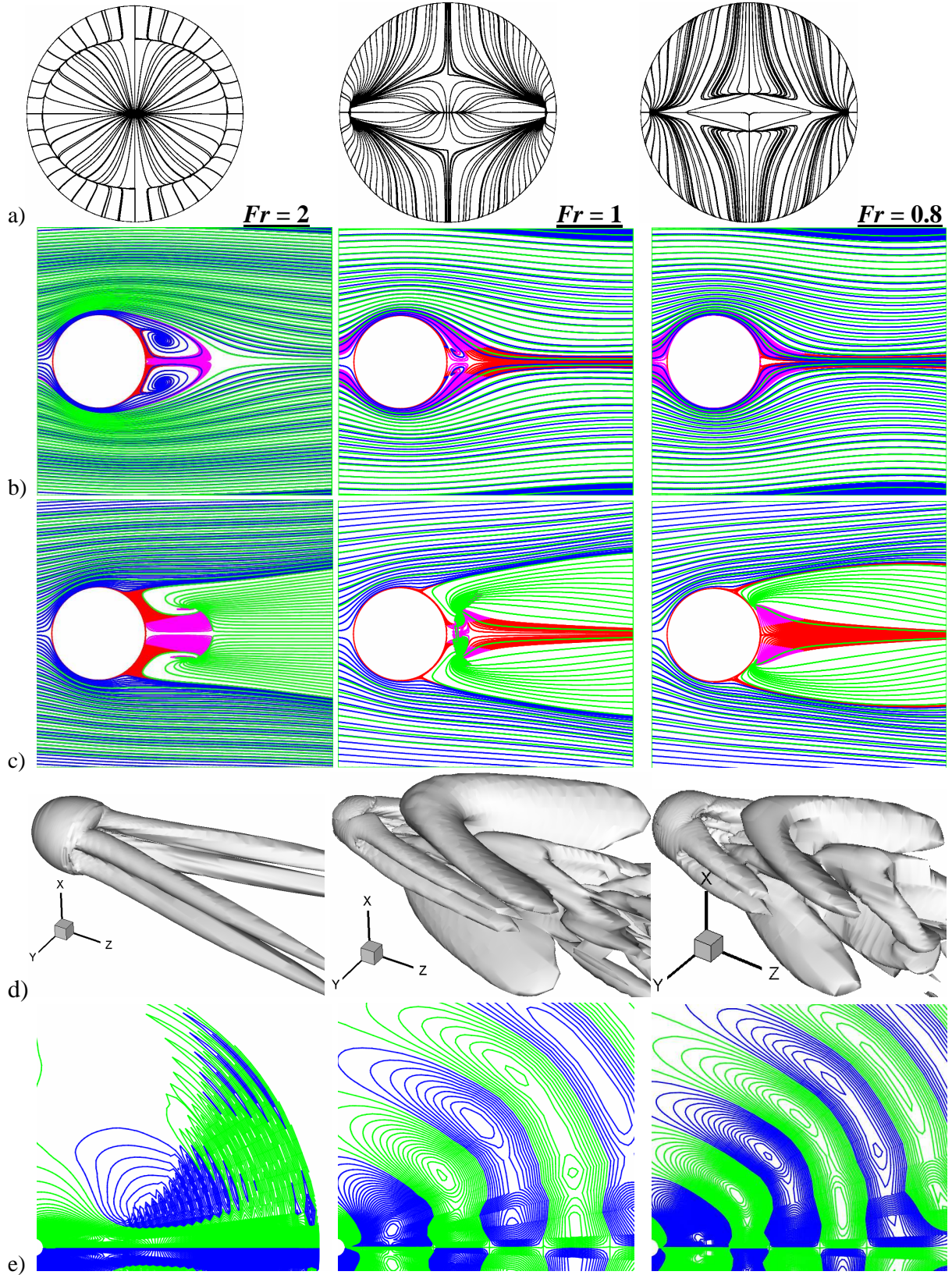
Figure 3: $Re = 100$, $Fr = 2, 1, 0.8$: a) the skin friction patterns on the sphere lee side; b-c) the stream lines in the vertical (b) and horizontal (c) planes; d) the isosurfaces of $\beta = 0.055, 0.02, 0.05$ [12]; e) the isolines of the perturbation of the salinity S ($dS = 5 \cdot 10^{-6}$ is the distance between the isolines), the darker isolines correspond to negative S.

For example for $200 < Re \leq 270$, $Fr = 2$ the six-threads wake is observed (fig. 4b). The domination of the four additional threads is obvious here. Unlike $Fr = 100$ at $Fr = 2$ ($200 < Re \leq 270$) the unsteadiness in the form of the periodical fluctuation of the rear stagnation point around axis Z is observed. Thus with decreasing of Fr (from 10 to 2) the vortex ring is deformed in an oval (Fig. 3a, 4b). In the vertical plane the part of fluid is supplied in the recirculation zone (fig. 3b). Then this fluid goes through the core of the vortex oval and is emitted downstream in the horizontal plane (fig. 3c). The 3D instantaneous stream lines which are going near the sphere surface go around this vortex oval and form the four vortex threads (Fig. 3d).
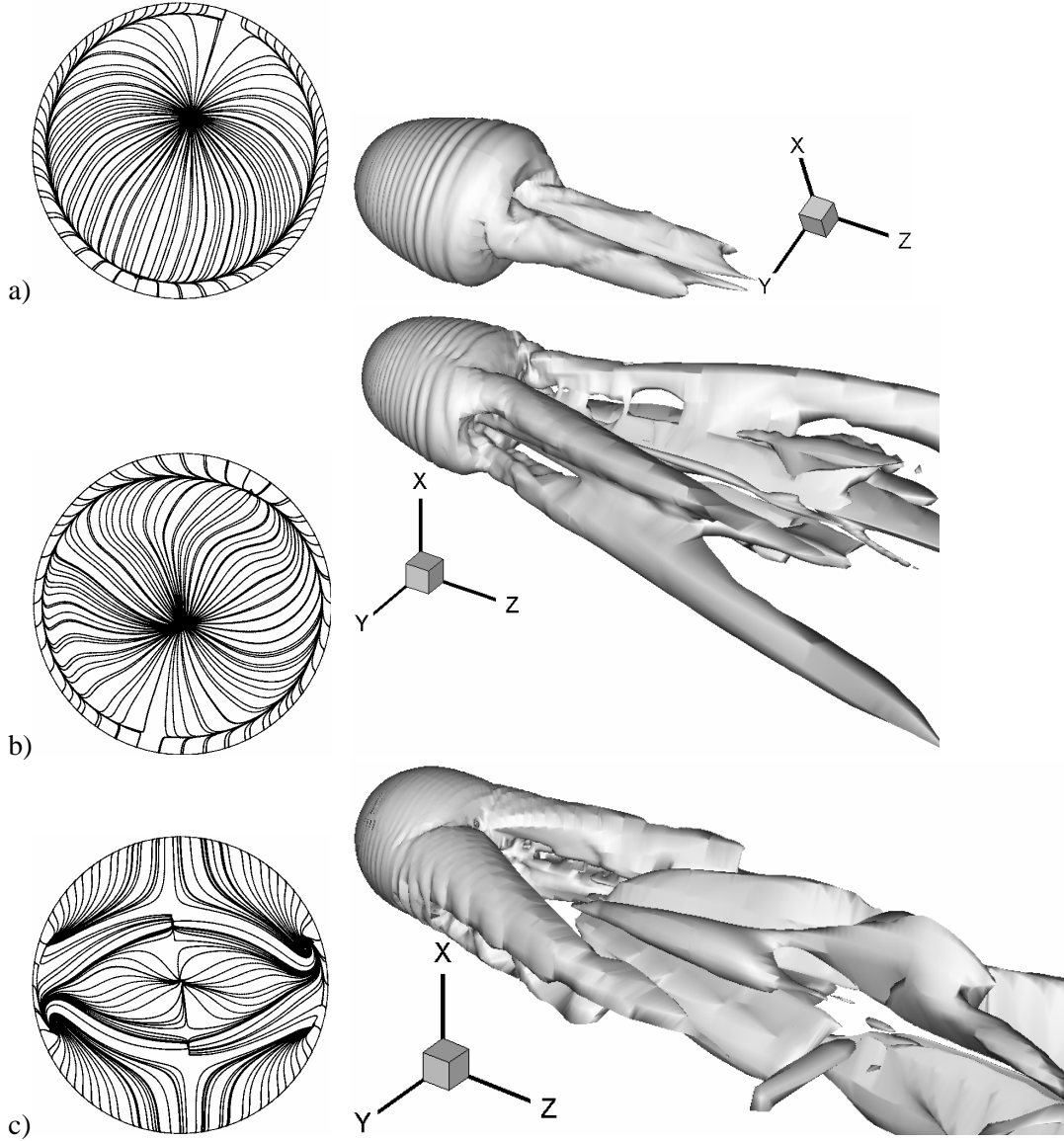

Figure 4:   The skin friction patterns on the sphere lee side (left fig.) and the isosurfaces of β [12] at $Re = 250$:
a) $Fr = 100$ (β = 0.04),   b) $Fr = 2$ (β = 0.04 – six threads),   c) $Fr = 1$ (β = 0.08).

At $Fr < 1.5$ ($200 < Re \leq 500$) the big initial vertical flattening of the flow (fig. 3a, 4c) prevent the vortex formation mechanisms typical for the homogeneous fluid. At $Fr < 1.5$ the new vortex formation mechanisms (which are typical for the stratified fluid) are realised with increasing of Re. With decreasing of Fr the fluid structures around the sphere are slowly flattened both along the vertical axis X (fig. 3a-b) and along the line of the sphere motion

(along axis *Z*, fig. 3c) (the length of the internal waves in the vertical plane is $\lambda/d \approx 2\pi \cdot Fr$ (fig. 5)). For example two free foci in fig. 3c are approaching to the sphere with decreasing of *Fr*. The length of four threads (connected with the vortex sheet surrounding the sphere at fig. 1, 3d, 4) is also diminished with reducing of *Fr* (fig. 6) and at $Fr \leq 0.1$ these threads are transformed in the *high gradient sheets of density* before the sphere (fig. 6 c-d).
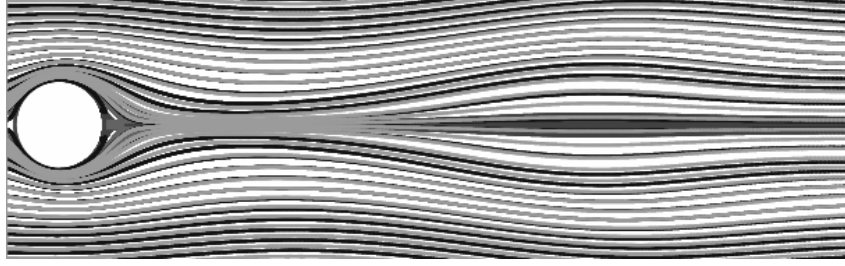

Figure 5: The stream lines in the vertical plane for $Fr = 1$, $Re = 100$.

During the **flow regime III** ($0.9 < Fr < 1.5$ – "*the non-axisymmetric attached vortex* in the recirculation zone", fig. 1, 3, 4c) the vortex oval in the recirculation zone has been transformed into the quasi-rectangle with two shot vertical vortex tubes (fig. 7c). With decreasing of *Fr* the thickness of this quasi-rectangle in the vertical plane *X-Z* is diminishing up to zero and this quasi-rectangle is transformed into the system of *the two symmetric vortex loops* (fig. 7d). It means that the wave processes destroy the rectangular vortex in the recirculation zone. As you can see from fig. 3d, 4c the top and bottom parts of each wave crest along the axis *Z* (fig. 5) are visualized as two symmetrical V-shaped vortex structures with the sloping ends. The head of this V-shaped vortex structure is connected with the four auxiliary vortex threads induced near the *Z* axis by the four main vortex threads (connected with the vortex sheet surrounding the sphere). In one's turn these four induced vortex threads are connected with the horizontal arc-shaped vortex structures represented the internal waves.

During the **flow regime IV** ($0.6 < Fr \leq 0.9$ – "the two symmetric vortex loops in the recirculation zone") the legs of these two symmetric vortex loops are combined with four induced vortex threads (mentioned above) (fig. 7d-e) and the primary separation line (and the recirculation zone) vanish. Thus at $0.4 \leq Fr \leq 0.6$ the **flow regime V** ("*the absence* of the recirculation zone") is observed (fig. 6a).

With decreasing of *Fr a new recirculation zone* is generated from the nearest wave crest at $Fr = 0.4$. During the **flow regime VI** ($0.25 < Fr < 0.4$ – "*a new recirculation zone*", fig. 6b, 7f) the V-shaped vortex structures are transformed into "dorsals". At $Fr \leq 0.25$ (with decreasing of *Fr*) these "dorsales" are shifted more close to the sphere and form a strong vortex envelope ("skeleton") around the new recirculation zone (fig. 6c). Thus at $Fr \leq 0.25$ the **flow regime VII** ("*the two vertical vortices* in the new recirculation zone (bounded by the internal waves)") is observed. At $0.03 \leq Fr \leq 0.25$ (at $Re < 120$) the ring-like primary separation line has been simulated (Fig. 6c). At $Fr < 0.03$ (at $Re < 120$) the cusp-like primary separation line with four singular points (two nodes (in *X-Z* plane) and two saddles (in *Y-Z* plane)) has been observed.

At $Fr \leq 0.3$, $Re > 120$ the edges of two vertical vortex sheets (on each side of the quasi-2D recirculation zone) are detached alternatively (fig. 6d). The corresponding Strouhal numbers $0.19 < St = f \cdot d/U < 0.24$ (where *f* is the frequency of shedding) are in a good agreement with the experiment [2].

The obtained characteristics of the simulated flows (such as horizontal and vertical separation angles, the drag coefficients) for $Fr \leq 100$, $Re \leq 500$ are in a good agreement with the experiments [1]-[2], [15]-[16].
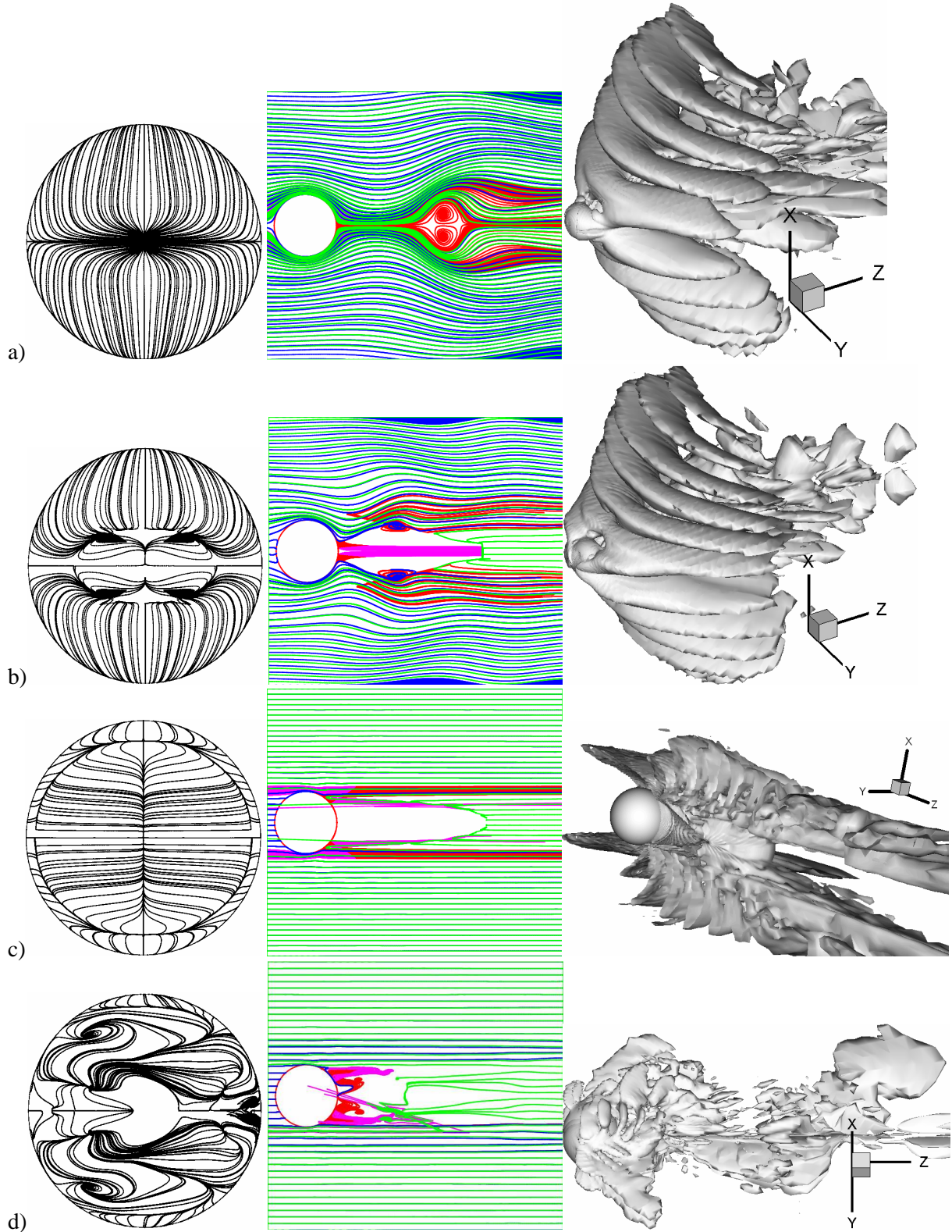
Figure 6: The skin friction patterns on the sphere lee side (left fig.), the stream lines in the vertical plane and the isosurfaces of β [12] (right fig.): a) $Fr = 0.5$, $Re = 100$ ($β = 0.02$), b) $Fr = 0.3$, $Re = 100$ ($β = 0.02$), c) $Fr = 0.08$, $Re = 100$ ($β = 0.005$), d) $Fr = 0.05$, $Re = 500$ ($β = 0.2$).
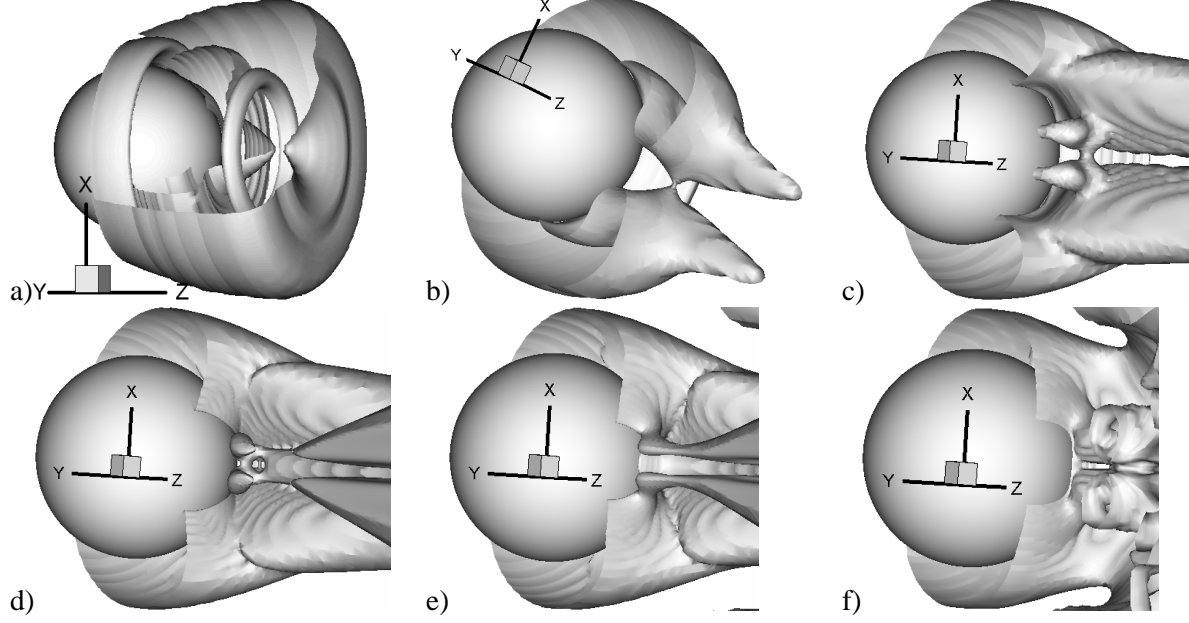
Figure 7: The isosurfaces of β [12] at *Re* = 100: a) *Fr* = ∞, b) *Fr* =2 (β = 0.15), c) *Fr* = 1 (β = 0.1),
d) *Fr* = 0.7 (β = 0.087), e) *Fr* = 0.6 (β = 0.087), f) *Fr* = 0.35 (β = 0.087).

5   CONCLUSIONS

The continuous changing of the complex 3D sphere wake vortex structure of the stratified viscous fluid with decreasing of *Fr* from 100 to 0.004 has been investigated at *Re* < 500 (*for the first time*) owing to the mathematical modelling on the massive parallel computers with a distributed memory and the β-visualization of the 3D vortex structures (the internal waves and the sphere wake). The numerical method SMIF and the β-visualization technique are briefly described. At 0.6 < *Fr* < 1.5 the gradual disappearance of the recirculation zone is observed (fig. 7). It is the most interesting and complex transformation of the wake vortex structure. At *Fr* = 0.4 a new recirculation zone is formed from the nearest "wave crest" which is appeared very close to the sphere.

With increasing of *Re* (from 100 to 500) the number of the degrees of freedom of the flow is increased too. At the same time the stratification stabilizes the flow in the sphere wake. As a result of our DNS at 0.004 ≤ *Fr* ≤ 100 and *Re* ≤ 500 the following classification of the flow regimes around a sphere horizontally moving in the viscous stratified fluid has been observed:
I) *Fr* > 10 – *the homogeneous case*, fig. 4a, 7a;
II) 1.5 ≤ *Fr* ≤ 10 – *the quasi-homogeneous case* (with four additional threads connected with the vortex sheet surrounding the sphere, fig. 1, 3d, 4b, 7b);
III) 0.9 < *Fr* < 1.5 - *the non-axisymmetric attached vortex* in the recirculation zone (fig. 1, 3d, 4c, 7c);
IV) 0.6 < *Fr* ≤ 0.9 – *the two symmetric vortex loops in* the recirculation zone, fig. 1, 3d, 7d;
V) 0.4 ≤ *Fr* ≤ 0.6 – *the absence* of the recirculation zone, fig. 6a, 7e;
VI) 0.25 < *Fr* < 0.4 – *a new recirculation zone*, fig. 6b, 7f;
VII) *Fr* ≤ 0.25 - *the two vertical vortices* in the new recirculation zone (bounded by the internal waves), fig. 6c-d.

This classification is more close to the classification from [1].

REFERENCES

[1] J.M. Chomaz, P. Bonneton and E.J. Hopfinger, The structure of the near wake of a sphere moving horizontally in a stratified fluid. *J. Fluid Mechanics*, **254**, pp. 1-21 (1993)

[2] Q. Lin, W.R. Lindberg, D.L. Boyer and H.J.S. Fernando, Stratified flow past a sphere. *J. Fluid Mech.*, **240**, pp. 315-354 (1992)

[3] Yu.D. Chashechkin, Hydrodynamics of a sphere in a stratified fluid. *Fluid Dynamics*, **24** (1), pp. 1-7 (1989)

[4] H. Hanazaki, A numerical study of three-dimensional stratified flow past a sphere. *J. Fluid Mech.*, **192**, pp. 393-419 (1988)

[5] D.C. Fritts, L. Wang, J. Werne, T. Lund and K. Wan, Gravity wave instability dynamics at high Reynolds numbers, 1: Wave field evolution at large amplitudes and high frequencies. *J. Atmos. Sci.*, **66**, pp. 1126-1148 (2009)

[6] V.A. Gushchin and V.N. Konshin, Computational aspects of the splitting method for incompressible flow with a free surface. *Journal of Computers and Fluids*, **21** (3), pp. 345-353 (1992)

[7] V.A. Gushchin and P.V. Matyushin, Numerical simulation of separated flow past a sphere. *Computational Mathematics and Mathematical Physics*, **37** (9), pp. 1086-1100 (1997)

[8] V.A. Gushchin, A.V. Kostomarov, P.V. Matyushin and E.R. Pavlyukova, Direct Numerical Simulation of the Transitional Separated Fluid Flows Around a Sphere and a Circular Cylinder. *Jnl. of Wind Engineering & Industrial Aerodynamics*, **90/4-5**, pp. 341-358 (2002)

[9] P.V. Matyushin, Numerical simulation of 3D separated homogeneous incompressible viscous fluid flows around a sphere. *Ph.D. Thesis*, Institute for Computer Aided Design Russian Academy of Sciences (in Russian) (2003)

[10] V.A. Gushchin, A.V. Kostomarov and P.V. Matyushin, 3D Visualization of the Separated Fluid Flows. *Journal of Visualization*, **7** (2), pp. 143-150 (2004).

[11] V.A. Gushchin and P.V. Matyushin, Vortex formation mechanisms in the wake behind a sphere for $200 < Re < 380$. *Fluid Dynamics*, **41** (5), pp. 795-809 (2006)

[12] M.S. Chong, A.E. Perry and B.J. Cantwell, A general classification of three-dimensional flow field. *Phys. Fluids*, **A 2** (5), pp. 765-777 (1990)

[13] V.G. Baydulov, P.V. Matyushin and Yu.D. Chashechkin, Structure of a diffusion-induced flow near a sphere in a continuously stratified fluid. *Doklady Physics*, **50** (4), pp. 195-199 (2005)

[14] V.G. Baydulov, P.V. Matyushin and Yu.D. Chashechkin, Evolution of the diffusion-induced flow over a sphere submerged in a continuously stratified fluid. *Fluid Dynamics*, **42** (2), pp. 255-267 (2007)

[15] K.E.B. Lofquist and L.P. Purtell, Drag on a sphere moving horizontally through a stratified liquid. *J. Fluid Mech.*, **148**, pp. 271-284 (1984)

[16] P.J. Mason, Forces on spheres moving horizontally in a rotating stratified fluid. Geophys. Astrophys. *Fluid Dyn.,* **8**, pp. 137-154 (1977)